Analysis of biogas reforming process for molten carbonate fuel cells

V. Chiodo, F. Urbani, A. Galvagno, N. Mondello, S. Freni*

CNR–ITAE "Nicola Giordano", Via S. Lucia sopra Contesse, 5–98126 - Messina, Italy

ARTICLE INFO

ABSTRACT

The paper reports the main results of an investigation on biogas reforming process developed for an integration with high temperature fuel cells systems. Experimental activities have been developed to determine performances of a nickel catalyst in different biogas reforming conditions have been investigated. Attention has been addressed toward the effect of gasifier agents (CO_2, H_2O and O_2) on outlet stream composition and carbon deposition on catalytic surface. Previously, the carbon formation rate in dry and steam reforming reactions apply to a biogas stream (CH_4/CO_2–60/40 vol%) has been evaluated using Aspen plus chemical processor simulator in order to define the operative conditions limit and to selected the best one.

A mathematical model, based on experimental data, has been developed to compare the polarization curves of a MCFC mono-cell fed with three different syngas compositions obtained by biogas reforming section in order to find out the best operational conditions for the two integrated systems (MCFC/fuel processor). A parallel trend of the the polarization curves have been obtained due to the assumptions considered for the model developing, as: (i) inlet gas composition effects on ohmic and activation loses are negligible; (ii) diffusional losses are dependent by gas compositions; (iii) diffusional losses are negligible in the graphic sections characterized by low current density.

© 2012 Elsevier B.V. All rights reserved.

1. Introduction

The need to improve air quality is one of the reasons that enhances interest of researchers towards a hydrogen economy. Several research initiatives were undertaken in the last decade to develop efficient systems to produce hydrogen from various raw sources [1–4]. In this context the hydrogen production from biomass, which is considered a CO_2 neutral energy source, has attracted particular attention. Biomass, either agricultural by-products or residual forest, which is abundantly available in the world, can be converted directly by gasification processes into syngas, however, it might also be interesting to consider the possibility to convert biomass into biogas, by fermentation process.

The term "biogas" defines a gaseous mixture, constituted basically of CH_4, CO_2, H_2S (<3 vol%) and traces of NH_3, obtained as a final product by anaerobic digestion of organic products. Reactions that take place in this process are grouped into the following stages, hydrolysis, acetogenesis and methanogenesis. The composition and characteristics of the biogas depend on the raw material (agricultural wastes and stockbreeder, the organic part of the urban and industrial solid waste and wastewater) as well as on the technology used.

Anyway, the most important biogas components are approximately 60% methane and 40% carbon dioxide [5–8]. Due to the presence of CO_2, the biogas is mainly used in a low-efficiency way, such as combustion in ICE or boilers. But, its potential use in fuel cells could represent a way to increase its conversion efficiency and reduce NOx emissions to the atmosphere. In particular, high-temperature fuel cells, i.e., solid oxide fuel cells (SOFC) and molten carbonate fuel cells (MCFC) offer the peculiarity of being able to tolerate the presence of impurities in the fuel, more than other fuel cell technologies [9–11]. However, in order to operate FCs supplied by biogas, a reformer section have to be designed in order to convert the biogas into a hydrogen rich gas mixture. This last process is affected by some problems that remain to be solved. First the presence of S- and N-containing compounds can readily poison the used catalysts. In principle, these harmful contaminants could be effectively removed from biogas before reforming stage by using conventional technologies [12–14].

The second factor is related to the carbonaceous deposition and in this direction, several studies have been addressed to test transition metal based catalysts (e.g., Ni, Ru, Rh and Pd) for the CO_2 reforming of CH_4 [15–20]. Among them, nickel is the most practical catalyst due to its low cost [21–24]. Recently, several researchers have used O_2 and/or steam for removing deposited coke on catalysts and both processes were reported to be able to restore and/or to limit the catalytic deactivation of Ni-based catalysts [25,26,5,27–31].

* Corresponding author. Tel.: +39 090 624230.
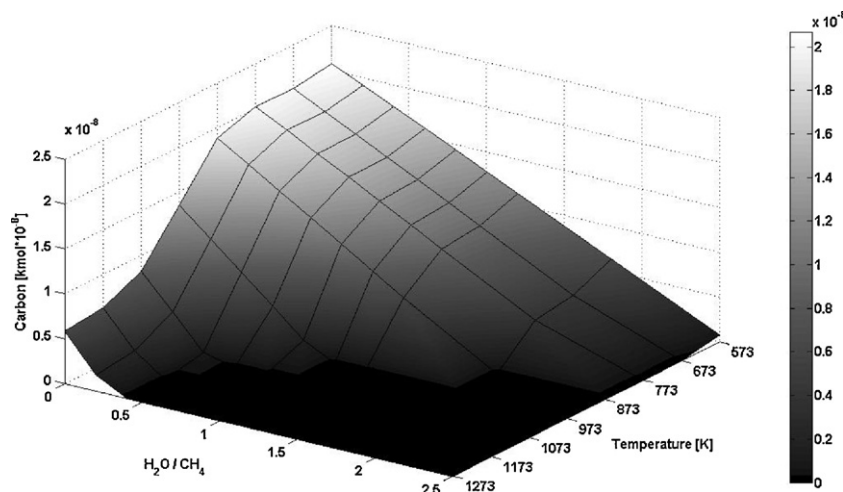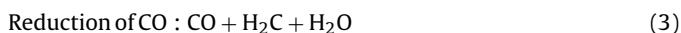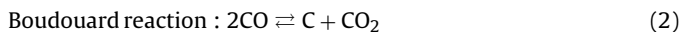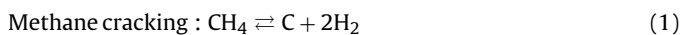E-mail address: salvatore.freni@itae.cnr.it (S. Freni).

Fig. 1. Effect of steam-carbon ratio and temperature on theoretical carbon formation rate.

Environmental benefits of using MCFC to produce electricity from alternative fuels has been reported in previous studies [32]; moreover, a commercial nickel catalyst has been reported as an highly promising material for carbon free reforming of hydrocarbon compounds [4,32,33]. On the basis of these experiences and considering the impressive efforts addressed towards the development of MCFCs, a wide investigation has been carried out to evaluate the potential use of biogas as a fuel for these systems. In particular, the conversion of biogas (CH_4–CO_2 = 60–40%) and the effects of steam and oxygen as gasifier agent have been explored with respect to carbon formation rate and H_2 selectivity. The process performance under thermodynamic and kinetic conditions were analyzed with respect to major operational parameters: oxygen/carbon and steam/carbon ratios.

2. Thermodynamic findings

Catalytic biogas reforming process is, generally, affected by the risk of carbon formation, especially at low H/C ratio. The carbon deposition is mainly consequence of one:

$$\text{Methane cracking}: CH_4 \rightleftarrows C + 2H_2 \qquad (1)$$

$$\text{Boudouard reaction}: 2CO \rightleftarrows C + CO_2 \qquad (2)$$

$$\text{Reduction of CO}: CO + H_2 C + H_2O \qquad (3)$$

Reactions (2) and (3) are not significant in coke formation at high temperature, while reaction (1) is favorable. It is well known that by increasing the H/C ratio in the reactor feed, the carbon formation rate will decrease due to a shift in the equilibrium of reaction (1) [33].

Therefore, as first step, to understand the mechanisms leading the reforming process of biogas, the theoretical carbon formation rate has been calculated by using Aspen Plus^{TM} chemical process simulator. In particular, the reforming reactions were modeled by using Gibbs reactor and minimizing the free energies in order to calculate the mole of carbon produced at a given conditions. The input data adopted for such a calculations were: (i) a simulated biogas consisting of 60% CH_4 and 40% CO_2; (ii) reagents inlet flow temperature; (iii) reactor temperature; (iv) reactor pressure equal to 1 bar.

Fig. 1 depicts the thermodynamic molar carbon concentration ranging the temperature from 573 K to 1273 K and the steam to carbon ratio from 0 mol mol^{-1} to 2.5 mol mol^{-1}. It is evident that in dry reforming condition (S/C = 0) a significant amount of elemental carbon could be formed for all range of considered temperatures. On the contrary, the addition of steam to CH_4–CO_2 mixture drastically changes the products equilibrium composition with carbon practically disappearing from the products at high temperatures (>923 K) and H_2O/CH_4 molar ratio higher than 0.5 mol mol^{-1}. In particular, the coking boundary in the steam biogas reforming reactions moves toward lower S/C values as the reactor temperature is raised. For example, if the reactor temperature is increased from 873 K to 1073 K, the coking boundary moves from a S/C of 2 to 1 mol mol^{-1}. These results demonstrate that the formation of solid carbon can be avoided by increasing the reactor temperature and/or the S/C ratio.

3. Experimental

3.1. Catalytic tests

On the basis of theoretical results showed in Fig. 1, catalytic performances of dry (DR), steam (SR), partial oxidation (POX) and autothermal reforming (ATR) of a simulated biogas stream (CH_4–CO_2 = 60–40%) were investigated at 1073 K and high GHSV value (150,000 h^{-1}), in order to evaluate the activity and stability of the catalyst. On the basis of earlier experiences, for these tests, it has been used a commercial Ni/Al$_2$O$_3$ catalyst (G56-A, SUD-CHEMIE AG, Munchen) [4,29,30]. The G56-A catalyst is mainly composed by 15 wt% of Ni supported on α-Al$_2$O$_3$ (63 wt%) and CaO (5.5 wt%) mixture whit traces of other constituents (i.e., SiO$_2$, Na <1 wt%).

All catalytic experiments (see Table 1) were performed, at atmospheric pressure, in a quartz fixed-bed linear micro-reactor (i.d. = 4 mm; H$_{bed}$ = 2.0–4.0 cm) loading 0.02–0.2 g of catalyst (grain size: 40–70 mesh) blended into similar sized inert material (SiC) with a dilution ratio, from 1:1 to 1:10, selected in order to have negligible temperature gradient in the bed. The reactor was placed into a furnace whose temperature (1073 K) was leaded by a controller driven by one thermocouple placed in a thermowell centred in the

Table 1
Operative conditions used in catalytic reforming tests.

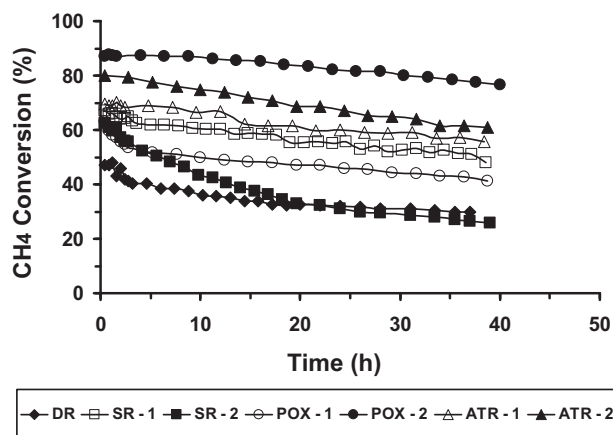|	$\left(\frac{H_2O}{CH_4}\right)_{in}$ (mol mol^{-1})	$\left(\frac{O_2}{CH_4}\right)_{in}$ (mol mol^{-1})	GHSV (10^3 h^{-1})
DR			150
SR-1	1.2		15–150
SR-2	2.5		150
POX-1		0.12	150
POX-2		0.25	15–150
ATR-1	1.2	0.06	150
ATR-2	1.2	0.12	15–150

Fig. 2. Methane conversion as a function of time on stream: $T = 1073$ K, GHSV = 150,000 h^{-1}.

catalyst bed. Additional thermocouples (two) were located at the inlet and outlet of the catalytic bed to measure gas temperature. The heating apparatus was calibrated is such a way that all temperature measuring points have the same constant temperature.

Before each test run, catalysts were reduced "in situ" at $T = 1073$ K for 1 h under hydrogen flow.

The feed flow rate of the simulated biogas ($CH_4 + CO_2$) and oxygen were controlled by mass flow meter, while the H_2O flow was fed by an isocratic HP 1100 pump and vaporized in a stainless steel reactor held at 493 K. Experiments were performed at $T = 1073$ K (constant) with a methane gas hourly space velocity (GHSV$_{CH_4}$ = catalyst bed volume/volume feed rate = $[m^3\,m^{-3}\,h^{-1}]$) of 150,000 and 15,000 h^{-1}, steam to carbon (mol mol^{-1}) $1.2 < S/C < 2.5$, calculated as mol of H_2O_{in}/mol of CH_{4in} in the inlet gas composition, and oxygen to carbon (mol mol^{-1}) $0.06 < O_2/C < 0.25$ (mol of O_{2in}/mol of CH_{4in}), molar ratios. The reaction stream was analyzed "on line" by a gas chromatography Hewlett–Packard (GC-HP model 6890 Plus), equipped with a three-columns (Molecular Sieve 5A, Porapak QS and Hysep Q) system and a thermal conductivity detector (TCD). Nitrogen (10 vol%) was used as an internal standard to evaluate the carbon balance. GC data were acquired and elaborated by the Hewlett–Packard Interface Bus system (HP Chemstation).

3.2. Catalyst characterization

TEM analyses were made by using a Philips CM12 instrument equipped with a high resolution camera that allows acquisition and evaluation (i.e., of the particle size distribution) of TEM images. Specimens were prepared by ultrasonic dispersion of catalyst samples into isopropyl alcohol and then a drop of suspension was deposited on a Formvar carbon grid Cu 400.

The overall amount of deposited carbon on the catalytic surface after each run test has been determined by CHNS elemental analysis of the discharged sample performed by Carlo Erba Elemental Analyzer. The samples were treated at high temperature in air and the CO_2 produced by oxidation was determined by a high sensitivity TC detector.

4. Results and discussion

As shown in Fig. 2, experiments carried out at high space velocity (150,000 h^{-1}) depict that under DR condition, the measured conversions were 47.12% with respect to CH_4 and about 75% for the CO_2. When steam was added until to reach 1.2 molar ratio of steam/carbon (SR-1), CH_4 conversion increased rapidly from
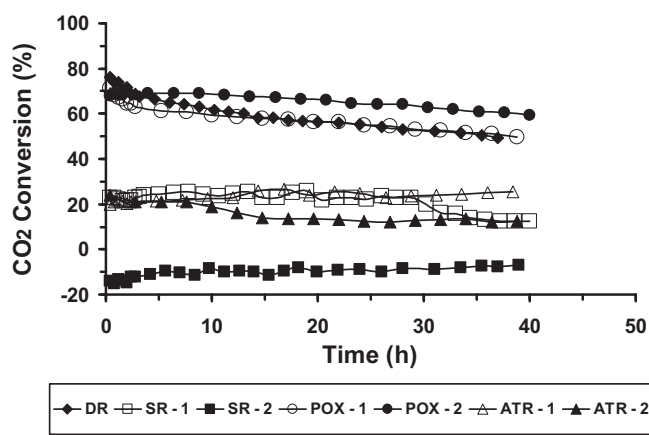
47.12% to 66%. However, adding more steam into feed gas composition (SR-2) a conversion rate very close to SR-1 (63%) was detected, moreover an evident catalytic deactivation was observed. Successively, oxygen effect was tested in absence or presence of steam in to biogas inlet composition and the catalytic performances evidenced a further increasing of methane conversion rate. In particular, under POX conditions with O_2/CH_4 ratio of 0.25 mol mol^{-1} (POX-2), it was achieved a CH_4 conversion of about 87%, while a lower O_2/CH_4 ratio (POX-1) leaded a conversion pattern very close to SR-2. On the contrary, for both ATR run tests, an enhancement of methane conversion if compared to DR and SR operative conditions was detected; about 69% and 77% for ATR-1 and ATR-2, respectively.

Results obtained in terms of CO_2 conversion (Fig. 3) depicts three different consume patterns. CO_2 conversion rate was the highest for DR and POX experiments (63.1% and 59;69% after 10 h for DR and POX-1;POX-2, respectively) but progressively decreased to about 22% in SR-1 and ATR experiments and it even became negative (-15%) in SR-2.

From the hydrogen yield point of view (Fig. 4), expressed as mol of H_{2out}/mol of CH_{4in}, the DR condition showed the lowest H_2 yield (about 1 mol mol^{-1}), while this parameter was the highest obtained (2.7 and 1.9 mol for ATR-2 and ATR-1 respectively) when simultaneously steam and oxygen were supplied in the inlet gas composition. H_2 yield of about 2 mol mol^{-1} was recorded for POX and SR conditions, even if for SR-2 a decrease with time was recorded while for POX-1 a significantly reduction of hydrogen production rate was highlighted (about 1.1 mol mol^{-1} after 10 h).

The above results suggest that the addition of a moderate amount of steam in the inlet gas composition favors
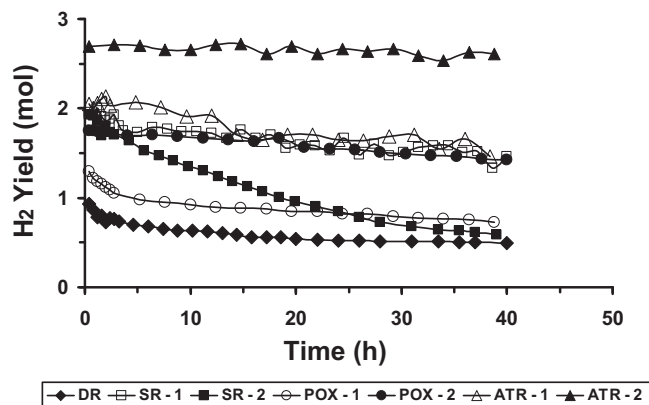

Fig. 3. Carbon dioxide conversion as a function of time on stream: $T = 1073$ K, GHSV = 150,000 h^{-1}.

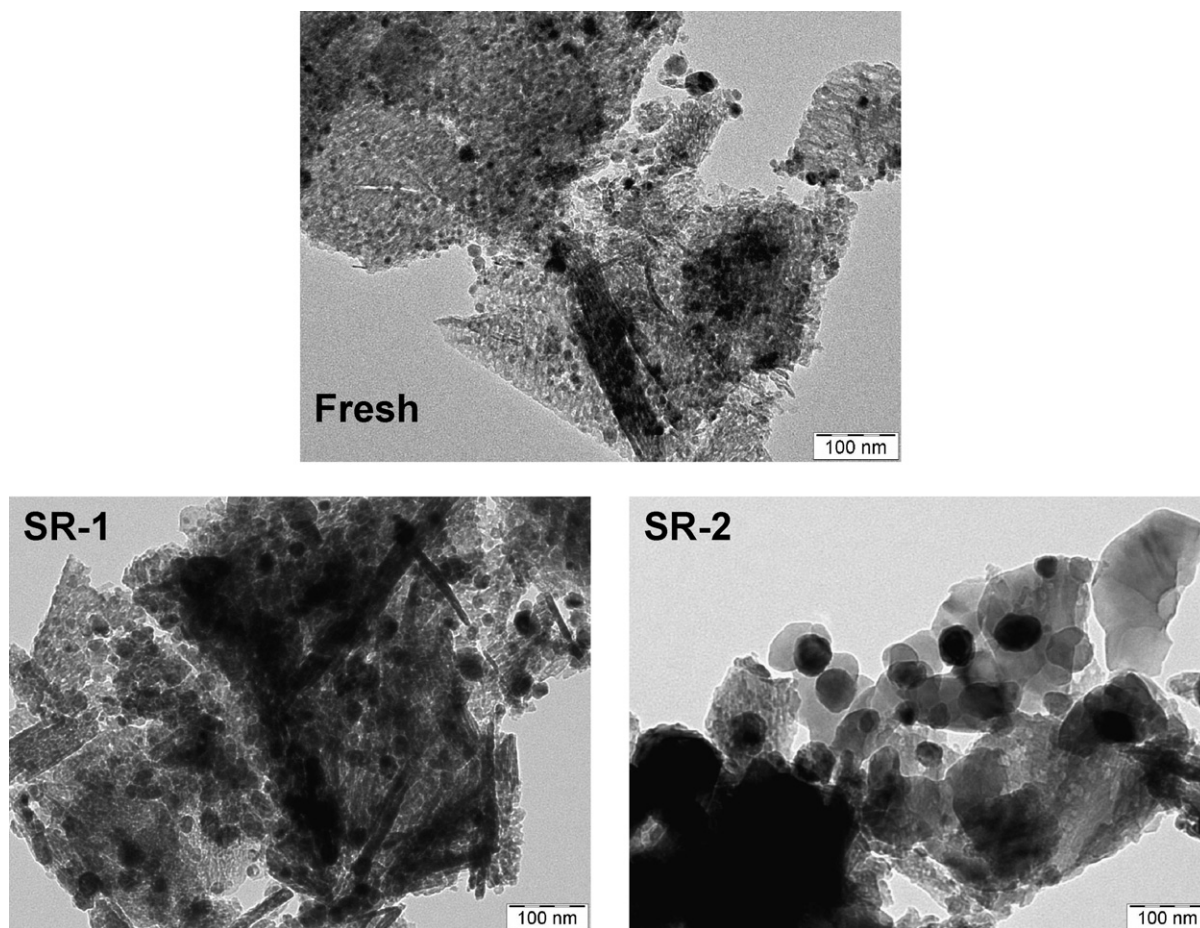**Fig. 4.** Hydrogen yield as a function of time on stream: $T = 1073$ K, GHSV = 150,000 h^{-1}.

Fig. 5. TEM images of fresh and used SR-1 and SR-2 samples: $T = 1073$ K, GHSV = 150,000 h^{-1}.

($S/C = 1.2$ mol mol^{-1}) the SR of methane but disadvantages the conversion of CO_2.

This means that methane can react with water prior to with carbon dioxide and it indicates that the CO_2 reforming (DR reaction) would be depressed by the steam presence, probably because the water gas shift reaction would be facilitates, leading to the increase of methane conversion and hydrogen production (see Fig. 4) [5]. These results suggest that the presence of steam in the inlet gas composition increases appreciably the biogas reforming process. Nevertheless, a further increase of S/C ratio (SR-2) did not show an increase of methane conversion. According to literature data, this behavior confirms that, at high temperature (>1023 K) and GHSV rate, CH_4 conversion remains practically constant and independent from S/C [34]. Anyway, SR-2 experiments showed, also, an evident catalytic deactivation trend, that appeared contrary to thermodynamic calculation. To shed light on this behavior, SR used samples were analyzed by TEM and CHNS elementary analysis (Figs. 5 and 6).

As evident from TEM micrographs, reported in Fig. 5, the Ni catalyst used in SR-2, show a growing of metal particles, in agreement with literature about sintering effect on Ni catalysts apply in biogas steam reforming processes when an excessive S/C inlet ratio [35,36] was used. This effect does not seem to be occurred on SR-1 catalyst sample, where Ni crystallites result to be in size almost close to those of the fresh catalyst sample. It can be drown conclusion that a sintering effect was promoted on SR-2 sample (increasing of particles diameter from 20 nm to 46 nm). This hypothesis has confirmed by: (i) no evident traces of carbon deposition were observed on catalytic surface by TEM images, (ii) low carbon formation rate

detected for each SR samples used by CHNS analysis; about 3 and 2.3 mgC $gcat^{-1}$ h^{-1}, for SR-1 and SR-2, respectively (Fig. 6).

Comparing the effect of oxygen on biogas reforming process in absence (POX) and in presence of steam (ATR) with SR-2, it can be observed that all catalytic performances presented a good stability for 40 h of run test. In particular, in POX experiments, the conversion of CH_4 increased with the addition of oxygen with almost
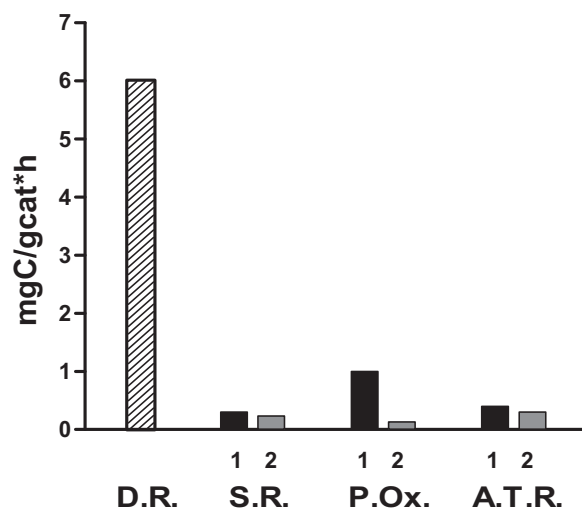

Fig. 6. Carbon formation rate on "used" samples: $T = 1073$ K, GHSV = 150,000 h^{-1}.

Table 2
MCFC inlet gas composition: $T = 1073$ K, GHSV = 15,000 h^{-1}.

	STR (%)	ATR (%)	POX (%)
H_2	53.6	49.7	48.3
CO_2	6	8.8	3.9
H_2O	9	15.3	4.1
CH_4	0.4	0.1	0.7
CO	31	26.1	43

88% conversion reached at O_2/CH_4 ratio of 0.25 mol mol^{-1} (POX-2). This tendency is probably due to the strong oxidizing proprieties of oxygen that facilitates the methane dissociation reaction and promotes CH_4 conversion and H_2 production [29,30]. However, the addition of O_2 at low O_2/CH_4 ratio (POX-1) has a negative effect on the H_2 yield although the CH_4 conversion is increased (Fig. 2), as compared to DR test. This could be attributed to dry reforming reaction that becomes more significant at this experimental conditions (high GHSV and temperature) promoting H_2O and CO_2 formation instead of H_2 as confirmed by CO_2 conversion rate (see Fig. 3) [37].

Catalytic performance carried out in ATR conditions showed that CH_4 conversion increased with O_2/C ratio, moreover higher CH_4 conversion values were depicted than SR operative conditions, while lower rates resulted with respect to POX-2. About H_2 yield, ATR-2 showed the best catalytic performance while ATR-1 gave a hydrogen production rate very close to SR-1 and POX-2 conditions. This result suggests that the oxygen presence in ATR-1 has not much effect on catalytic performance, probably because the O_2/CH_4 ratio was very low, indeed both CH_4, CO_2 conversions and H_2 yield were close to SR-1. On the contrary, ATR-2 performance data suggests the co-existence of small amounts of steam and oxygen increase H_2 formation rate if compared to other reforming reactions. It should be noted that throughout all POX and ATR tests, the conversion of O_2 remained constant to 100%.

In order to compare how biogas reforming process is influenced by process conditions, a comparison has been done in terms of carbon formation rate on spent catalysts. Results, showed in Fig. 6, indicate that a significant carbon deposition occurs on surface of used catalyst, under DR conditions (about 6 mgC gcat^{-1} h^{-1}), with higher rate than that observed in the other experiments. On the other hand, the carbon formation could be eliminated in presence of steam and/or oxygen in the inlet gas composition. In particular, POX conditions seem to be better operative condition for biogas processing, mainly when a $O_2/CH_4 = 0.25$ mol mol^{-1} ratio was adopted (0.11 mgC gcat^{-1} h^{-1}). At the same time, both SR-1 and ATRs experiments, according to thermodynamic calculation, drastically inhibited the carbon formation.

On the basis of the results obtained in terms of carbon formation on Ni catalyst, three experimental tests (SR-1; POX-2; ATR-2) were performed at low GHSV (15,000 h^{-1}), in order to obtain the product molar fractions under thermodynamic conditions. Results presented in Table 2 where CH_4 conversion was about 98% for all tests and no carbon formation was detected on samples used catalyst (after 40 h).

5. MCFC system configuration

The very high operating temperatures of molten carbonate and solid oxide fuel cells make them particularly suitable for biogas usage. In fact, the presence of CO in syn-gas (up to 40%) [37], produced by biogas reforming, that is a harmful gas for low temperature fuel cells, represents an improvement factor if used in high temperature FC. Besides, the high temperature of the FC outlet gas allows the gas-processing unit to be thermal integrated with the power section.

In our study, whose main results are reported in this paper, a Molten Carbonate Fuel Cell supplied by a syn-gas production process, like as described in the earlier section, was selected and calculations to determine the best operational conditions for the two integrated systems (MCFC/fuel processor) have been carried out.

This choice was made because systems based on MCFC are, among the high temperature fuel cell systems, in an advanced stage of market penetration (i.e., Fuel Cell Energy system).

In Molten Carbonate Fuel Cell the following half-reactions occur at the anode (Eqs. (4) and (5)) and at the cathode (Eq. (6)):

$$H_2 + CO_3^{2-} \rightarrow CO_2 + H_2O + 2e^- \tag{4}$$

$$CO + CO_3^{2-} \rightarrow 2CO_2 + 2e^- \tag{5}$$

$$2CO_2 + O_2 4e^- \rightarrow 2CO_3^{2-} \tag{6}$$

The stoichiometry of Eqs. (4) and (5) show that the anodic outlet is enriched with CO_2 according to the conversion of the reactants and the cathodic outlet is depleted by the same amount of CO_2 [38]. The concentrations of outlet products in syn-gas are changing as a function of the production process as described in the previous paragraphs.

In order to evaluate the influence induced by syn-gas production process to be coupled to a MCFC, a mathematical model has been developed.

The equilibrium fuel cell potential (V_{eq}) in terms of temperature and gas compositions is given by the Nernst equation (Eq. (7)):

$$V_{eq} = E_0 + \frac{RT}{2F} \ln \left[\frac{p_{H_2 an} \; p_{O_2 cat}^{0.5} \; p_{CO_2 cat}}{p_{H_2 an} \; p_{CO_2 an}} \right] \tag{7}$$

The Nernst equation gives the relationship between the ideal standard potential (E_0), depending on the overall cell reaction, and the ideal equilibrium potential, depending on local conditions of temperature and partial pressures (p_k) of reactants and products.

During electricity production, fuel cell voltage is affected by irreversible losses, caused by: (i) electrochemical dynamic limitations; (ii) activation polarization; (iii) mass transport limitations; (iv) resistive ohmic effect.

Losses can be estimated by calculating the three primary voltage drops of activation, concentration, and Ohmic polarizations. So the operating cells voltage (V_{cell}) can be estimated by Eq. (8):

$$V_{cell}(I) = V_{eq} - V_{act}(I) - V_{Ohm}(I) - V_{conc}(I) \tag{8}$$

where V_{act} is the activation overvoltage, V_{conc} is the concentration overvoltage, V_{Ohm} is the Ohmic voltage drop and I is the current density. Polarization losses are generally dependent on gas partial pressures, temperature, and current density, all of which are spatially distributed in the cell.

To find out the best composition to integrate syn-gas processor unit to MCFC ones, it was decided to compare the polarization curve (as a function of current density obtained from Eq. (8)) for a MCFC monocell fed with different syn-gas compositions, that have been previously and experimentally obtained, as shown in the previous paragraph. The trend of losses (V_{act}, V_{Ohm} and V_{conc}) at different current densities has been obtained taking into account experimental data on a single cell MCFC by 94 cm^2 obtained from experimental tests already carried out [39].

In the calculations of polarization curves it has been assumed that: (i) as reported by Wolf et al., ohmic losses are not influenced by inlet gas compositions [40]; (ii) as reported by Wilemski, the influence of the inlet syn-gas composition on activation losses is negligible, whereas the differences in inflows composition is not likely to induce a significant error [41]; (iii) diffusional losses, dependent by gas compositions, assume significant values in the section of curve characterized by high values of current densities;
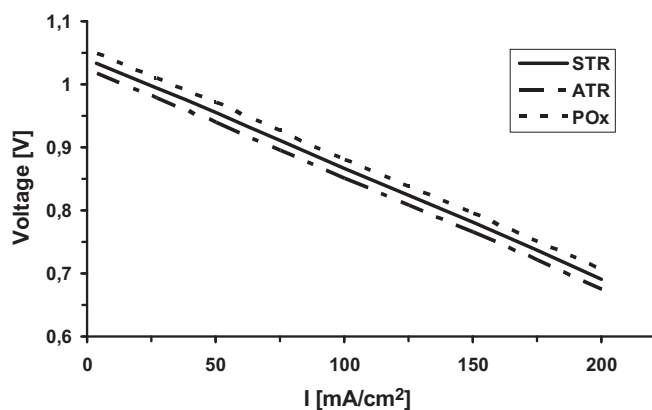
Fig. 7. MCFC polarization curves: $T = 923$ K, $p = 1$ bar.

(iv) diffusional losses are negligible in the other graphic sections; this does not correspond to reality, but considering that the composition of syn-gas produced by different gas-processing unit have a similar composition, leads to the conclusion that the error is negligible and does not affect particularly the comparison made; (v) the cathode gas composition is assumed equal to a stream composed by 75% air and 25% CO_2.

Starting from the known outlet syn-gas compositions (Table 1), determined as a function of the selected gas-processing unit, by using these ones as values of partial pressure in Eq. (7), we calculated the value of V_{eq} and reported in Fig. 6 the polarization curves so established.

As it is evident, the polarization curves are parallel, owing to the simplification made, because of the curve slope is defined from the overvoltage. From Fig. 7 it appears that the partial oxidation is the most efficent syn-gas production process to be integrated to MCFC systems. In fact, as shown by the comparison of the data in Table 2, the best polarization curve is defined by the syn-gas with a lower concentration of both water and carbon dioxide. These products, that appear in the denominator of Nernst's equation, will contribute to a cell voltage increasing when their concentration will be lower. Anyway, in the examined case, the voltage gain will be partially lost due to the effect of lower hydrogen concentration that shows an opposing trend. As conclusion, the overall effects of reactants concentration variation will produce an overall positive effect on the Nernst cell voltage.

6. Conclusions

The technical feasibility of syn-gas produced by biogas use reformer for feeding a molten carbonate fuel cell was analytically and experimentally evaluated.

A thermodynamic analysis has been carried out conducted in order to determine the theoretical carbon formation rate leading by biogas reforming process. Therefore, favorable operating conditions have been determined to reform biogas without carbon formation. These operative conditions have been adopted to carried out catalytic tests at 1073 K in DR, SR, POX and ATR at different ratios of S/C and/or O_2/C and different GHS Velocities.

Experimental data evidenced that, in the investigated range of operative conditions, the suitable S/C ratio, under SR, was 1.2 mol mol^{-1}, moreover, it was highlighted that an excessive presence of steam seems to be harmful for catalytic stability in the test carried out at 1073 K and 150,000 h^{-1}. At the same time, results depicted that, the appropriate conditions for biogas POX process include oxygen on methane ratio of 0.25 mol mol^{-1}, while in ATR conditions, the most favorable oxygen and steam on carbon ratios were 1.2 and 0.12 for S/C and O_2/C, respectively. Furthermore,

the best performance in terms of methane conversion has been detected for POX system, but compared to ATR experiments it produced a lower H_2 yield. Anyway, the difference in terms of H_2 yield between SR (S/C = 1.2 mol mol^{-1}), POX (O_2/C = 0.25 mol mol^{-1}) and ATR (S/C = 1.2 mol mol^{-1} and O_2/C = 0.12 mol mol^{-1}) was quite negligible.

Results in terms of carbon formation rate indicated that biogas reforming under DR condition is affected by a mechanism of carbon deposition (about 6 mgC gcat^{-1} h^{-1}). On the other hand, carbon formation rate could be drastically reduced in presence of steam and/or oxygen in the inlet gas composition. In particular, POX conditions seem to be the most suitable biogas process, mainly when a O_2/CH_4 = 0.25 mol mol^{-1} ratio was used (0.11 mgC gcat^{-1} h^{-1}).

Successively, the most promising outlet gas stream composition obtained by the different biogas reforming processes conditions were selected and used to calculate the polarization curves of a MCFC. Results indicated that partial oxidation reforming gives syngas with such a composition that makes it as the most convenient to be integrated with high temperature fuel cells.

References

[1] M. Ball, M. Wietschel, Int. J. Hydrogen Energy 34 (2009) 615–627.
[2] D.B. Levin, R. Chahine, Int. J. Hydrogen Energy 35 (2010) 4962–4969.
[3] M.A. Pena, J.P. Gómez, J.L.G. Fierro, Appl. Catal. A: Gen. 144 (1996) 7–57.
[4] V. Chiodo, S. Freni, A. Galvagno, N. Mondello, F. Frusteri, Appl. Catal. A: Gen. 381 (2010) 1–7.
[5] P. Kolbitsch, C. Pfeifer, H. Hofbauer, Fuel 87 (2008) 701–706.
[6] M. Harasimowicz, P. Orluk, G. Zakrzewska-Trznadel, A.G. Chmielewski, J. Hazard. Mater. 144 (2007) 698–702.
[7] I.V. Yentekakis, J. Power Sources 160 (2006) 422–425.
[8] J. Huang, R.J. Crookes, Fuel 77 (1998) 1793–1801.
[9] A.A. Iordanidis, P.N. Kechagiopoulos, S.S. Voutetakis, A.A. Lemonidou, I.A. Vasalos, Int. J. Hydrogen Energy 31 (2006) 1058–1065.
[10] P. Leone, A. Lanzini, M. Santarelli, M. Calì, F. Sagnelli, A. Boulanger, A. Scaletta, P. Zitella, J. Power Sources 195 (2010) 239–248.
[11] R. Bove, P. Lunghi, J. Power Sources 145 (2005) 588–593.
[12] M. Syed, G. Soreanu, P. Falletta, M. Béland, Canadian Biosyst. Eng. 48 (2006).
[13] M. Ashrafi, C. Pfeifer, T. Proll, H. Hofbauer, Energy Fuels 22 (2008) 4190–4195.
[14] N. Abatzoglou, S. Boivin, Biofuels Bioprod. Bioref. 3 (2009) 42–71.
[15] J.R. Rostrup-Nielsen, Catal. Today 4 (1993) 305–324.
[16] J.H. Edwards, A.M. Maitra, Fuel Process. Technol. 42 (1995) 269289.
[17] X. Chen, K. Honda, Z.-G. Zhang, Catal. Today 93–95 (2004) 87–93.
[18] K. Diaz, V. Garcia, J. Matos, Fuel 86 (2007) 1337–1344.
[19] Q. Jing, H. Lou, J. Fei, Z. Hou, X. Zheng, Int. J. Hydrogen Energy 29 (2004) 1245–1251.
[20] F. Pompeo, N.N. Nichio, O.A. Ferretti, D. Resasco, Int. J. Hydrogen Energy 30 (2005) 1399–1405.
[21] S. Xu, X.L. Wang, Fuel 84 (2005) 563–567.
[22] S.X. Xu, X.L. Yan, X. Wang, Fuel 85 (2006) 2243–2247.
[23] F. Pompeo, D. Gazzoli, N.N. Nichio, Int. J. Hydrogen Energy 34 (2009) 2260–2268.
[24] S. Therdthianwong, A. Therdthianwong, C. Siangchin, S. Yongprapat, Int. J. Hydrogen Energy 33 (2008) 991–999.
[25] T. Zhang, M.D. Amiridis, Appl. Catal. A: Gen. 72 (1998), 167–161.
[26] G.F. Froment, J. Mol. Catal. A: Chem. 163 (2000) 147–156.
[27] A. Effendi, K. Hellgardt, Z.G. Zhang, T. Yoshida, Fuel 84 (2005) 869–874.
[28] V.R. choudhary, B.S. Uphade, A.S. Mamman, Appl. Cat. A: Gen. 168 (1998) 33–46.
[29] N. Muradov, F. Smith, A. Ti-Raissi, Int. J. Hydrogen Energy 33 (2008) 2023–2035.
[30] D. Sun, X. Li, S. Ji, L. Cao, Natural Gas Chem. 19 (2010) 369–374.
[31] M.H. Halabi, M.H.J.M. de Croon, J. van der Schaaf, P.D. Cobden, J.C. Schouten, Chem. Eng. J. 137 (2008) 568–578.
[32] F. Urbani, S. Freni, A. Galvagno, V. Chiodo, J. Power Sources 196 (2011) 2691–2698.
[33] N. Palmeri, V. Chiodo, S. Freni, F. Frusteri, J.C.J. Bart, S. Cavallaro, Int. J. Hydrogen Energy 33 (2008) 6627–6634.
[34] M. Ashrafi, T. Proll, C. Pfeifer, H. Hofbauer, Energy Fuels 22 (2008) 4182–4189.

[35] F.B. Rasmussen, J. Sehested, H.T. Teunissen, A.M. Molenbroek, B.S. Clausen, Appl. Catal. A: Gen. 267 (2004) 165–173.
[36] E. Acha, J. Requies, V.L. Barrio, J.F. Cambra, M.B. Guemez, P.L. Arias, Int. J. Hydrogen Energy 35 (2010) 11525–11532.
[37] C.S. Lau, A. Tsolakis, M.L. Wyszynskia, Int. J. Hydrogen Energy 36 (2011) 397–404.
[38] J. Brouwer, F. Jabbari, E.M. Leal, T. Orr, J. Power Sources 158 (2006) 213–224.
[39] S. Freni, M. Pons, A. Parmaliana, CNR-TAE Int. Rep. 06, 1988.
[40] T.L. Wolf, G. Wilemski, J. Electrochem. Soc. 130 (1983) 48–55.
[41] G. Wilemski, J. Electrochem. Soc. 130 (1983) 117–121.